IET Generation, Transmission & Distribution

Research Article

Use of demand response for voltage regulation in power distribution systems with flexible resources

ISSN 1751-8687
Received on 1st August 2019
Revised 13th November 2019
Accepted on 19th December 2019
E-First on 31st January 2020
doi: 10.1049/iet-gtd.2019.1170
www.ietdl.org

Qiangqiang Xie[1,2], Hongxun Hui[1], Yi Ding[1] ✉, Chengjin Ye[1], Zhenzhi Lin[1], Peng Wang[3], Yonghua Song[1], Ling Ji[4], Rong Chen[5]

[1]*College of Electrical Engineering, Zhejiang University, Hangzhou, People's Republic of China*
[2]*College of Electronics and Information, Hangzhou Dianzi University, Hangzhou, People's Republic of China*
[3]*School of Electrical & Electronic Engineering, Nanyang Technological University, Singapore*
[4]*Guodian Nanjing Automation Co., LTD, Nanjing 211100, People's Republic of China*
[5]*State Grid Zhejiang Electric Power Co., LTD, Zhejiang 310007, People's Republic of China*
✉ *E-mail: yiding@zju.edu.cn*

Abstract: In low-voltage power distribution systems with high penetration of photovoltaics (PVs) generation and electric vehicles (EVs), the over-voltage problem arises at times because of large PV generation, and under-voltage problem also arises sometimes because of simultaneous charging of massive EVs. Over- and under-voltage problems lead to more difficulties in achieving voltage regulation. Demand response (DR) is expected to be promising and cost-effective in promoting smart grids, and hence, the utilisation of flexible resources (FRs) through DR can be helpful for distribution system voltage regulation. This study introduces a hierarchical control structure of a community energy management system (CEMS) and multiple sub-CEMSs to apply an FR-based two-stage voltage regulation technique. In the first stage, i.e. the day-ahead scheduling stage, each sub-CEMS optimises the FRs' schedules for minimising customers' electricity cost and network voltage violation times. In the second stage, i.e. the real-time operation stage, the voltage sensitivity-based FRs' shifting method is proposed to eliminate network voltage violations caused by errors of estimated day-ahead data. The proposed models and methods are verified based on a realistic distribution system in Japan, where voltage violations, customer electricity cost and a number of on-load tap changer tap operations are proved to be reduced.

Nomenclature

Index

i,j	index of customer node number
t	time slot number
p	phase index $p \in \{a, b, c\}$

Parameters

A	appliances of FLs
C_{FIT}	FIT price
C_{buy}	electricity purchasing price
C_{sell}	electricity selling price
$I_{\mathrm{line}}^{ij,p}$	line current between i and j of phase p
$I_{\mathrm{line}}^{\mathrm{lim}}$	line current limit
N_A	total number of FLs
$V_{\min}$	voltage low limit
$V_{\max}$	voltage high limit
V_{sub}	rated secondary voltage magnitude of the substation transformer
η_{eff}	charging efficiency coefficient
$\boldsymbol{J}$	Jacobian matrix
l_{FL}	load of FL
l_{ODL}	load of ODL
N_{c}	set of all customer nodes except the substation node
$S_{\max}$	rated capacity of the PV inverter
Γ	set of all time slots
T	total number of time slots in a day
$\mathrm{Tem}_{\mathrm{in}}^{\mathrm{lowlim}}$	low limit of indoor temperature
$\mathrm{Tem}_{\mathrm{in}}^{\mathrm{highlim}}$	high limit of indoor temperature
tp	tap position of the OLTC
λ	weight coefficient in the objective function
$\mathrm{Cap_b}$	battery capacity
$\mathrm{SOC}_{\max}$	maximum EV SOC
$\mathrm{SOC}_{\min}$	minimum EV SOC
Δt	length of a time interval
γ	change ratio per step of OLTC
μ	thermal parameter of environment
ρ	thermal parameter of AC

Variables

$\boldsymbol{B}^{ij,p}$	imaginary part of the element in the bus admittance matrix of phase p
$\boldsymbol{G}^{ij,p}$	real part of the element in the bus admittance matrix of phase p
$P_{\mathrm{AC}}^{i,p}(t)$	power of AC of customer node $i$of phase p at time slot t
$P_{l_{\mathrm{FL}}}^{i,p}(t)$	active power of FL of customer node i of phase p at time slot t
$P_{l_{\mathrm{ODL}}}^{i,p}(t)$	active power of ODL of customer node i of phase p at time slot t
$P_A^{i,k}(t)$	power of kth appliance A at time slot t
$P_{\mathrm{EV}}^{i,p}(t)$	charging power of EV of customer node i of phase p at time slot t
$P_{\mathrm{EV}}^{\max}$	maximum charging power of EV
$P_{\mathrm{load}}^{i,p}(t)$\`	total load of customer i of phase p at time slot t
$P_{\mathrm{xch}}^{i,p}(t)$	active power exchange of customer i and DSO of phase p at time slot t
$Q_{\mathrm{PV},PF}$	reactive power under the PF limit
$Q_{\mathrm{PV},S}$	reactive power of PV
$Q_{\mathrm{PV}}^{i,p}(t)$	reactive power of PV inverter of the customer i of phase p at time slot t

$Q_{\mathrm{xch}}^{i,p}$	reactive power exchange of customer i and DSO of phase p at time slot t
$T_{A\_ot}^{k}$	minimum working time of kth appliance A
$T_{A\_\mathrm{start}}^{k}$	start time of kth appliance A
$\mathrm{Tem}_{\mathrm{in}}^{i,p}(t)$	indoor temperature of customer i of phase p at time slot t
$\mathrm{Tem}_{\mathrm{out}}^{i,p}(t)$	outdoor temperature of customer i of phase p at time slot t
$V^{i,p}$	voltages at customer node i of phase p
$V^{j,p}$	voltages at customer node j of phase p
Φ_{A}^{k}	feasible working interval of kth appliance A
Φ_{EV}^{i}	feasible charging and discharging interval of an EV
α_{A}^{k}	allowed starting time of the kth appliance A
$\alpha_{\mathrm{EV}}^{i,p}$	allowed starting time of EV of customer i of phase p
β_{A}^{k}	allowed finishing time of the kth appliance A
$\beta_{\mathrm{EV}}^{i,p}$	allowed finishing time of EV of customer i of phase p
$\delta^{ij,p}$	difference of voltage angle of customer i,j of phase p
$\psi_{\mathrm{buy}}(t)$	cost of customers who purchase electricity from the day-ahead market
$\psi_{\mathrm{FIT}}(t)$	profit from the FIT policy
$\psi_{\mathrm{sell}}(t)$	income of customers who sell electricity to the market
P_{PV}	active power of PV
$\boldsymbol{S}$	voltage sensitivity matrix
$SW_{A}^{i,k}(t)$	switch state of kth appliance A
$x(t)$	SOC of the battery
$\Delta P(t)$	required active power for voltage regulation
$\Delta Q(t)$	required reactive power for voltage regulation
$\Delta U(t)$	difference between the customers node voltage and the high or low limit

1 Introduction

The development of smart grids has changed the electric power distribution systems significantly in recent years [1]. The distributed generations, e.g. rooftop photovoltaic (PV) generations, are increasingly integrated into the electric power distribution systems. This probably causes the counter-flow of electric power from customers to the network, especially when the PVs' power generation is larger than the local load demand. More seriously, the distribution system voltage probably rises higher than the upper limit by the high penetration of rooftop PVs, which is named the over-voltage problem [2].

The electric vehicle (EV) technologies have been extensively developed for reducing the emission of greenhouse gases in many cities around the world [3], which causes load spike when massive EVs charge at the same time. It can make the distribution system voltage drop significantly and may lead to the voltage below the lower limit [4], causing under-voltage problems.

Generally, the over-voltage usually occur at mid-day when the PVs' power generation is extremely high, while the under-voltage problems occur at mid-night when most of residential customers charge their EVs. Therefore, distribution system operators (DSOs) must cope with the over- and under-voltage problems during different periods in a day.

Some studies have been performed to deal with voltage violation problems in distribution systems. For example, the on-load tap changer (OLTC) and the step voltage regulator are used to directly regulate the voltage by DSOs [5, 6]. However, the intermittent generation characteristics of PVs may cause frequent tap operations and decrease the lifetime of the OLTCs. Moreover, utilising the reactive power is another conventional method for regulating voltage in distribution systems [7], where the reactive power can be generated by shunt capacitors (SCs) [8], static var compensators (SVCs) [9], static synchronous compensators (STATCOMs) [10] for mitigating the voltage violations. However, more sources of reactive power are required for voltage regulation with rapidly increasing PVs and EVs. Mounting installation of SC, SVC and STATCOM are based on the high construction cost of corresponding infrastructures, which are not desirable.

PV inverters can absorb or inject reactive power, which is considered as reactive power sources [11, 12]. Besides, coordinated control of the above two methods (i.e. OLTCs and reactive power control methods) are also considered in [13–15] to improve the control effect, while the effectiveness of the reactive power in voltage regulation can be limited due to the large resistance/reactance ratio in the low-voltage distribution systems. Moreover, large reactive power flow in the low-voltage distribution systems will increase the line congestion and power losses [16], which are adverse to the economic operation of power systems.

With the development of information and communication technologies (ICTs) [17], smart meters are increasingly installed in residential households, making available of the bidirectional communication between customers and the system operator, which makes the demand response (DR) implementable [18–20]. On this basis, PVs, EVs and flexible loads (FLs) can be regarded as flexible resources (FRs) in distribution systems. The community energy management systems (CEMSs) have been developed in recent years to automatically schedule FRs with dynamic electricity price, and thus save the cost for customers [21]. This provides an alternative method to regulate the distribution system voltage by adjusting the active power in distribution systems [22]. For example, storage devices are used in [23] to regulate the system voltage. However, considering the large capacity requirements and corresponding expensive cost, this method is hard to deal with rapidly increasing PVs and EVs in the near future distribution systems.

PVs' active power curtailment is considered in [24, 25], while this method can lead to the reduction of solar energy utilisation. Moreover, the DR control algorithms for residential customers are proposed in [26] to shave the network peaks and solve under-voltage problems. Venkatesan *et al*. [27] propose a price elasticity matrix to guide electricity consumption for solving under-voltage problems. However, these methods usually suppose that household load controllers could respond to the price signals to modify the load schedules, which may be not effective if the residential customers at the voltage violation area do not respond to the dynamic electricity prices. As a result, it is better to schedule the FRs at the voltage violation nodes rather than sending the price signals to the residential customers.

Load scheduling by the DR scheme is proposed in [28], where the voltage regulation is achieved by keeping load demand below a certain limit during peak hours. This study points out that heuristic methods will be considered to solve the rebound effect in future work. O'Connell *et al*. [29] present a rolling optimisation to minimise the charging cost of EVs and regulate the voltage violation. The rolling optimisation is carried out at each 30-min time step for the subsequent 12-h window. Real-time coordination of OLTCs and schedulable loads is proposed in [30] to prevent the over-voltage problems, while the under-voltage problem is not considered. Ziadi *et al*. [31] propose a centralised day-ahead optimisation of FRs, OLTCs, step voltage regulators and PVs' reactive power output to deal with the over-voltage problem, while the model of FRs are built roughly and the characteristics of different FRs are not considered. Furthermore, few studies consider three-phase and unbalanced power flow, while distribution systems are usually unbalanced.

Facing the above challenges, this paper develops the model of residential FRs in low-voltage distribution systems to schedule them in three-phase unbalanced power distribution system, for solving the voltage violation problems. First, the hierarchical control structure considering the CEMS and multiple sub-CEMSs is proposed. On this basis, the two-stage FRs scheduling method is developed, including the day-ahead scheduling and real-time operation. The objective of the day-ahead scheduling is to minimise both distribution system voltage violation times and customers' cost. In the second stage of real-time operation, a voltage sensitivity-based FRs' shifting method is proposed to eliminate the network voltage violation caused by errors of estimated day-ahead data. The originality and contributions of this paper are as follows:

(i) A comprehensive DR strategy of FR scheduling is developed in three-phase unbalance power distribution systems to fully exploit the demand elasticity of FRs for providing voltage regulation services. The objectives include avoiding voltage violations, minimising customer electricity cost and decreasing OLTC tap operation times, which are proved to be beneficial to both customers and DSOs.
(ii) A decentralised control structure considering the coordination of CEMS and multiple sub-CEMSs is proposed, where time-consuming heuristic algorithms are used and achieved to solve the non-linear time-series optimisation of FRs in large-scale distribution systems.
(iii) A two-stage control method is first proposed to utilise FRs for providing voltage regulation services. In the first stage, i.e. the day-ahead scheduling stage, FRs are scheduled and optimised for minimising customers' electricity cost and voltage violation times. In the second stage, i.e. the real-time operation stage, a fast (average 0.017 s in the simulation) real-time operation method is developed to solve short-term voltage violations caused by PV output fluctuations or estimation errors.

The remaining part of this paper is organised as follows. Section 2 proposes the system architecture. The problem formulation and solution algorithm are presented in Section 3. Numerical evidence for the benefits of the proposed method is provided in Section 4. Finally, in Section 5 and Section 6 discussions and conclusions are provided, respectively.

2 Modelling of FRs-based voltage regulation system

2.1 System structure

The system structure of the proposed scheduling scheme for residential customers equipped with FRs is illustrated in Fig. 1. Traditionally, the power generated by PVs in the distribution system is less than the local power consumption, and therefore the power in the substation flows from the transmission line to the distribution system. With rapidly increasing construction of PVs, the power flow probably gets reversed, especially when the PVs generation is higher than the local demand during some periods (e.g. the power generation by PVs is extremely high at mid-day). The large reverse power flow will cause over-voltage problems in the distribution systems. Besides, the increasing number of household appliances and EVs can cause high peak loads if these devices consume power at the same time (e.g. most of EVs charge at night), which will cause under-voltage problems.

In the proposed model, the DSO, as the distribution system manager, forecasts the day-ahead data, performs the power flow analysis, and makes the day-ahead OLTC schedule. Although the OLTC is usually adjusted autonomously using traditional line-drop compensation, researchers have found that it does not work properly when the distribution system is installed with large-scale PVs [5, 6]. It is assumed that customers are installed with smart meters, and the voltage of customers can be observed. In this case, OLTCs can be scheduled by the DSO. The large-scale CEMS is separated into multiple sub-CEMSs. The sub-CEMS manages customers under the same pole transformer because these customers' voltages are highly correlated. The CEMS undertakes the coordinator, which receives power flow calculation results from the DSO and price signal from the electricity market, and then sends the primary node's voltage and price information to sub-CEMSs.

Each customer is equipped with a smart meter, which is used to achieve the two-way communications between the sub-CEMS and customers [18, 20]. The sub-CEMSs can optimise the loads' schedule of corresponding customers with two objectives, i.e. reducing the customers' electricity cost and distribution system voltage violation times. Customers can preset operating constraints for FRs to guarantee their comfort. The CEMS and sub-CEMSs can be seen as two-level DR aggregators [32], which assist customers to manage FRs to respond to the DR program for voltage regulation under dynamic electricity prices.

2.2 Modelling of distribution systems

The power flow of a radial power distribution system can be modelled and described as follows [33]:

$$V_0 = V_{\text{sub}}(1 + tp \cdot \gamma) \tag{1}$$

$$P_{\text{xch}}^{i,p} = V^{i,p} \sum_{j}^{N_c} V^{j,p}\left(\boldsymbol{G}^{ij,p}\cos\delta^{ij,p} + \boldsymbol{B}^{ij,p}\sin\delta^{ij,p}\right) \tag{2}$$

$$Q_{\text{xch}}^{i,p} = V^{i,p} \sum_{j}^{N_c} V^{j,p}\left(\boldsymbol{G}^{ij,p}\sin\delta^{ij,p} - \boldsymbol{B}^{ij,p}\cos\delta^{ij,p}\right) \tag{3}$$

$$\left|I_{\text{line}}^{ij,p}\right| < I_{\text{line}}^{\text{lim}} \tag{4}$$

The current $I_{\text{line}}^{ij,p}$ flowing through each distribution line should be under the current limit $I_{\text{line}}^{\text{lim}}$ in order to avoid overloading.

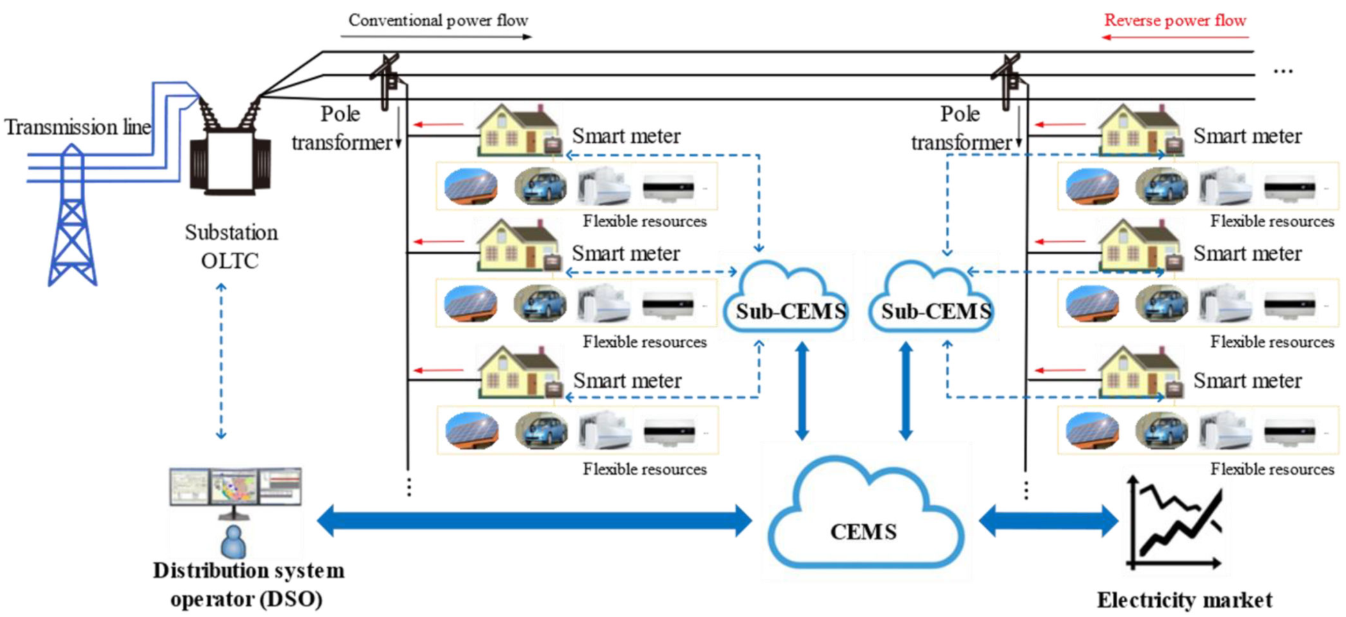

Fig. 1 *System architecture of the residential scheduling scheme*

2.3 Modelling of PV units

In recent years, many organisations have published numerous standards to introduce concepts that low voltage active customers can adjust their exchanged reactive power to provide ancillary services for power systems [34]. Thus, PV inverters can be designed for providing reactive power support for voltage regulations.

In this paper, the maximum power point tracking function is assumed to be provided in the PV unit. Thus, the constraint for controlling the PV's reactive power output without decreasing the active power generation can be represented as

$$-\sqrt{S_{\max}^2 - P_{\rm PV}^2} \le Q_{{\rm PV},S} \le \sqrt{S_{\max}^2 - P_{\rm PV}^2} \tag{5}$$

The PV's power factor (PF) can be calculated by

$$PF = \cos\left(\tan^{-1}\left(\frac{Q_{{\rm PV},S}}{P_{\rm PV}}\right)\right) \tag{6}$$

In distribution systems, the absolute value of the PF should be in a permissible range. The low absolute value of PF can increase power loss. Thus, the reactive power under the PF limit is given by

$$Q_{{\rm PV},PF} = \tan(\arccos(PF)) \cdot P_{\rm PV} \tag{7}$$

Let $\Gamma \triangleq \{1, 2, \ldots, t, \ldots, T\}$ denote the time slots of a day. The adjustable reactive power of customer-i's PV inverter of phase p at time slot t is

$$Q_{\rm PV}^{i,p}(t) = \min\left\{Q_{{\rm PV},S}^{i,p}(t) \quad , \quad Q_{{\rm PV},PF}^{i,p}(t)\right\} \tag{8}$$

2.4 Modelling of EVs

The dynamic model for the batteries of EVs is given by

$$x(t+1) = x(t) + \frac{\eta_{\rm eff} \cdot \Delta t}{{\rm Cap_b}} P_{\rm EV}(t) \tag{9}$$

Here, the efficiency coefficient $\eta_{\rm eff}$ is assumed to be constant regardless of the charging power according to [3].

The state of charge (SOC) should not exceed the minimum and maximum limits, which can be expressed as

$$\mathrm{SOC}_{\min} \le x(t) \le \mathrm{SOC}_{\max} \tag{10}$$

$\Phi_{\rm EV}^{i,p} \triangleq \left[\alpha_{\rm EV}^{i,p}, \beta_{\rm EV}^{i,p}\right]$ is defined as feasible charging and discharging periods of an EV. The charging state starts from $\alpha_{\rm EV}^{i,p}$, and the battery should be fully charged before $\beta_{\rm EV}^{i,p}$.

When $t \in \left[\alpha_{\rm EV}^{i}, \beta_{\rm EV}^{i}\right]$, the constraint of $P_{\rm EV}^{i,p}(t)$ is given by

$$\begin{cases} P_{\rm EV}^{i,p}(t) \in [0, P_{\rm EV,max}], & \mathrm{SOC}_{\min} \le x(t) \le SOC_{\max} \\ P_{\rm EV}^{i,p}(t) = 0, & \text{otherwise} \end{cases} \tag{11}$$

The EV should be fully charged before the deadline, as a result, the constraint of SOC before the deadline is given by

$$x(t) = \mathrm{SOC}_{\max}, \quad t = \beta_{\rm EV}^{i,p} \tag{12}$$

2.5 Modelling of air conditioners (ACs)

ACs are thermostatically controlled appliances, and the comfortable temperature should be ensured in order to avoid affecting customer's preference when ACs are utilised for DR. According to [28], the indoor temperature can be calculated by the outside temperature and operating power of ACs, as follows:

$$\begin{aligned} \mathrm{Tem}_{\rm in}^{i,p}(t) = & \ \mathrm{Tem}_{\rm in}^{i,p}(t-1) \\ & + \mu \cdot \left(\mathrm{Tem}_{\rm out}^{i,p}(t) - \mathrm{Tem}_{\rm in}^{i,p}(t-1) + \rho \cdot P_{\rm AC}^{i,p}(t)\right) \end{aligned} \tag{13}$$

where μ and ρ are thermal parameters of the environment and the AC, respectively. ρ is negative when the AC operates in cooling mode, while it is positive when the AC is in heating mode. Besides, the indoor temperature should not exceed the allowable variation ranges, which is expressed as

$$\mathrm{Tem}_{\rm in}^{i,p}(t) \in \left[\mathrm{Tem}_{\rm in}^{\rm lowlim}, \mathrm{Tem}_{\rm in}^{\rm highlim}\right] \tag{14}$$

When the indoor temperature is in the range between the high and low limits, the power consumption of the corresponding AC can be regulated and utilised for the voltage regulation. When the indoor temperature is higher than the upper limit, the AC has to return to operate.

2.6 Modelling of flexible loads

The residential electricity loads include on-demand loads (ODLs) $l_{\rm ODL}$ and $l_{\rm FL}$ [21, 35]. Examples of such ODLs include lights and televisions because their energy consumption usually cannot be scheduled easily. In contrast, the working period of FLs can be flexibly rearranged. For example, customers only care about whether the washing machine can finish the work before a specified deadline. The flexible scheduling of FLs can be used for voltage regulation.

Since the ODL cannot be scheduled, $P_{l_{\rm ODL}}^{i,p}(t)$ is assumed to be fixed for each customer at time slot t. On the other hand, $P_{l_{\rm FL}}^{i,p}(t)$ is a combination of several FLs, which can be expressed as

$$P_{l_{\rm FL}}^{i,p}(t) = \sum_{i=1}^{N_A} P_A^{i,k}(t) \cdot SW_A^{i,k}(t) \tag{15}$$

where $SW_A^{i,k}(t)$ denotes the status of the appliance, which is 1 to indicate that the A ($A \in l_{\rm FL}$) is in the working state, and 0 to indicate the off state, respectively.

Moreover, $\Phi_A^k \triangleq \left[\alpha_A^k, \beta_A^k\right]$ is defined as the allowable working interval for A, i.e. A should start to work after α_A^k and must finish its work before β_A^k. Thus, $P_A^{i,k}(t)$ can be described as

$$P_A^{i,k}(t) = \begin{cases} P_A^{i,k}, & T_{A\_\rm start}^k \le t \le T_{A\_\rm start}^k + T_{A\_\rm ot}^k \\ 0, & \text{others} \end{cases} \tag{16}$$

$$\alpha_A^k \le T_{A\_\rm start}^k \le \beta_A^k - T_{A\_\rm ot}^k \tag{17}$$

In summary, the total load of a customer i of phase p at time slot t can be evaluated as

$$P_{\rm load}^{i,p}(t) = P_{l_{\rm ODL}}^{i,p}(t) + P_{l_{\rm FL}}^{i,p}(t) + P_{\rm EV}^{i,p}(t) + P_{\rm AC}^{i,p}(t) \tag{18}$$

The power exchange of customer i and DSO of phase p at time slot t can be represented as

$$\begin{aligned} P_{\rm xch}^{i,p}(t) = & \ P_{\rm PV}^{i,p}(t) - P_{l_{\rm ODL}}^{i,p}(t) - P_{l_{\rm FL}}^{i,p}(t) \\ & - P_{\rm EV}^{i,p}(t) - P_{\rm AC}^{i,p}(t) \end{aligned} \tag{19}$$

Although FR includes a variety of devices, most of them can be modelled as a device that consumes a certain volume of energy in a specific time. The PV, EV and AC can be normalised as an inverter, a battery and a thermostatically controlled device, respectively. All of them consume a certain power under specific constraints, which have been considered above. As a result, the modelling of FRs in this study is generic enough, so that it can adapt to different appliances for providing DR.

3 Problem formulation

The proposed voltage regulation technique using FRs consists of day-ahead load scheduling and real-time operation. In the first stage, i.e. day-ahead scheduling, the start time of the FRs is optimised to minimise the electricity cost of the customers and voltage violation times of the distribution system. In the second stage, i.e. real-time operation, the voltage sensitivity-based FRs' shifting method is proposed to ensure the voltage within the permissible range.

3.1 Day-ahead FR scheduling model

In the day-ahead optimisation, the usage periods of FRs are determined according to the day-ahead electricity prices. As shown in Fig. 2, the CEMS receives the day-ahead price from the electricity market, and then sends to each sub-CEMS. Each sub-CEMS returns the tentative FRs schedule to the CEMS. The CEMS collects all the information and sends to the DSO. The DSO estimates the PV and ODL data of the next day through historical data. With the load data and estimated PV data, the DSO can decide the OLTC setting and carry out the power flow calculation of the distribution system. Finally, the DSO sends the voltage of pole transformers to the CEMS, and then the CEMS sends the specific primary node voltage to sub-CEMSs. Each sub-CEMS optimises the schedule of FRs considering the following two objectives: minimising both the electricity cost of its sub-system and the times of voltage violations. The mathematical formulations of each sub-CEMS are shown as follows:

$$\begin{aligned}\text{Min}\, F = \lambda \cdot \sum_{t=1}^{T} \left(\psi_{\text{buy}}(t) - \psi_{\text{sell}}(t) - \psi_{\text{FIT}}(t)\right) \\ +1 - \lambda \sum_{t=1}^{T} \sum_{p=a}^{c} \sum_{i=1}^{N_c} V_{vio}^{i,p}(t)\end{aligned} \tag{20}$$

$$\psi_{\text{buy}}(t) = -C_{\text{buy}} \cdot \frac{\Delta t}{60} \cdot \sum_{p=a}^{c} \sum_{i=1}^{N_c} P_{\text{xch}}^{i,p}(t), P_{\text{xch}}^{i,p}(t) < 0 \tag{21}$$

$$\psi_{\text{sell}}(t) = C_{\text{sell}} \cdot \frac{\Delta t}{60} \cdot \sum_{p=a}^{c} \sum_{i=1}^{N_c} P_{\text{xch}}^{i,p}(t), P_{\text{xch}}^{i,p}(t) \geq 0 \tag{22}$$

$$\psi_{\text{FIT}}(t) = \begin{cases} C_{\text{FIT}} \cdot \frac{\Delta t}{60} \cdot \sum_{p=a}^{c} \sum_{i=1}^{N_c} P_{\text{xch}}^{i,p}(t), & P_{\text{xch}}^{i,p}(t) > 0 \\ 0, & P_{\text{xch}}^{i,p}(t) \leq 0 \end{cases} \tag{23}$$

$$V_{vio}^{i,p}(t) = \begin{cases} 1, & V^{i,p}(t) > V_{\max}\ or\ V^{i,p}(t) < V_{\min} \\ 0, & V_{\min} \leq V^{i,p}(t) \leq V_{\max} \end{cases} \tag{24}$$

$$\text{subject to} (1) - (15) \text{ and}$$

$$Q_{\text{xch}}^{i,p}(t) = Q_{\text{load}}^{i,p}(t) + Q_{\text{PV}}^{i,p}(t) \tag{25}$$

where $\lambda \in (0,1)$ is a weight coefficient. In (20), the first part denotes the total electricity cost of all customers under the same sub-CEMS of the next day, while the second part is the total number of voltage violations of all customers' nodes. A larger λ in the objective function (20) will be more emphatic in minimising the electricity cost.

Genetic algorithm (GA) is utilised in this study to solve the aforementioned optimisation problem. The objective function of (20) includes two parts: minimising customers' electricity cost and minimising voltage violation times. The decision value is the start time of all FRs. In the initialisation of GA, the start time of FRs are randomly determined by obeying the constraints of $T_{A\_\text{start}}^{k} \in \left[\alpha_A^k, \beta_A^k - T_{A\_\text{ot}}^k\right]$, and then the initial population is formulated by the decision value. The fitness evaluation is carried by the calculation of objective function. The power of FRs during

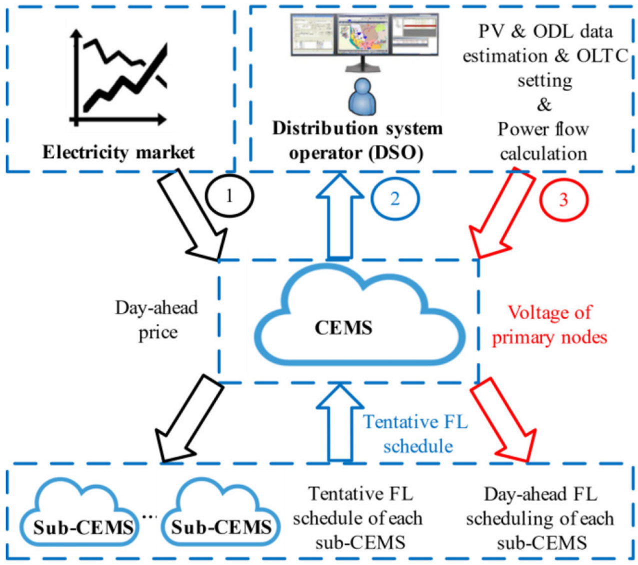

Fig. 2 *Flow chart of the day-ahead scheduling*

the working span is calculated from the start time by programming. Thus, the customer electricity cost and the number of voltage violations can be determined. Next, the roulette wheel algorithm is used for the chromosomes selection. The signal-point algorithm is applied for the crossover. In the process of mutation, some genes are replaced by a randomly generated start time $T_{A_i}^{\text{start}'}$. Subsequently, a new population is generated, and the GA repeats the process until the pre-defined generation is reached.

We also consider the day-ahead scheduling of the OLTC operation. Since the operation speed of OLTCs is slow in the power distribution system, and frequent tap changing should be avoided. However, the setting of the OLTC and the scheduling of FRs can both affect the power flow of the distribution system. It is difficult and time consuming to optimise the setting of OLTC and the simultaneous scheduling of FRs in one GA optimisation. In this study, after each sub-CEMS decided the scheduling of FRs in step 3 of Fig. 2, it sends the load scheduling data to the DSO. The DSO decides the OLTC operation to eliminate all the voltage violations. Since the voltage violation minimisation is considered in the optimisation in step 3, it will help the OLTC to reduce the operation times. The changing of OLTC's setting will change the primary node voltage. Therefore, each sub-CEMS will optimise the FRs scheduling again for minimising the cost by considering the voltage constraints, which can be expressed as

$$\text{Min} \sum_{t=1}^{T} \left(\psi_{\text{buy}}(t) - \psi_{\text{sell}}(t) - \psi_{\text{FIT}}(t)\right) \tag{26}$$

$$V_{\min} \leq V^{i,p}(t) \leq V_{\max} \tag{27}$$

3.2 Real-time operation model

After the day-ahead optimisation, the start time of the FRs is decided by the sub-CEMS in order to minimise the electricity cost and voltage violation times. However, the day-ahead schedule includes estimation errors of PVs and ODLs. Voltage violations may still occur because of these errors. Thus, real-time operation of FRs is necessary for guaranteeing voltage in the permissible ranges. In the real-time operation, each sub-CEMS observes the voltage profile of its covering system with following the day-ahead schedule.

When over-voltage occurs, the adjustable reactive power of PV inverter is first utilised to decrease the voltage deviations. If all the adjustable reactive power has been used and the over-voltage still cannot be regulated, a combination of un-started FRs will be deployed to decrease the voltage. By contrast, when the under-voltage occurs, a combination of FRs which can be delayed will be turned off to raise the voltage.

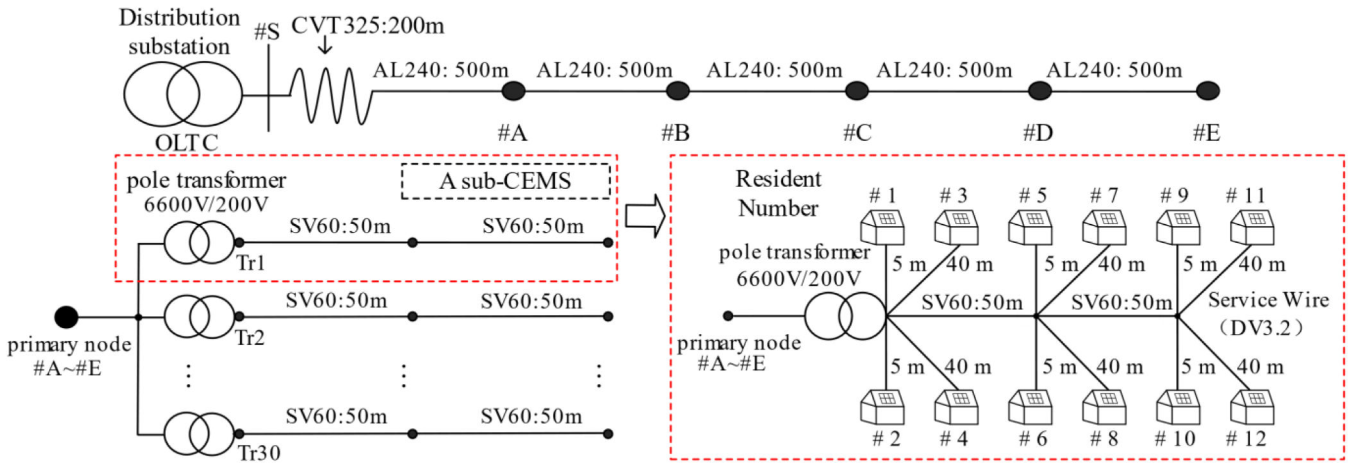

Fig. 3 *Distribution system model with 1800 customers*

Table 1 FR Specifications

	A_k	$[\alpha_{A_k}, \beta_{A_k}]$	$T^{\text{ot}}_{A_k}$, min	P_{A_k}, kW
1	rice cooker	6:00–8:00	45	1
2	ventilator	0:00–24:00	60	0.5
3	washing machine	0:00–24:00	60	0.7
4	AC	—	—	2
5	rice cooker	9:00–11:00	45	1
6	rice cooker	15:00–18:00	45	1
7	dish washer	20:00–24:00	45	0.6
8	EV	18:00–6:00	360	3

Since the power flow is non-linear, the operation of different appliances at different customer node i can produce different voltage regulation effects. Voltage sensitivity method is an effective way to decide the location and amounts of reactive and active power to serve the voltage regulation. The sensitivity matrix $\boldsymbol{S}$ is derived from the system Jacobian matrix in solving the non-linear load flow by the Newton–Raphson algorithm [10]. The $\boldsymbol{S}$ matrix is the inverse of the Jacobian matrix

$$\begin{bmatrix} \Delta\theta \\ \Delta U \end{bmatrix} = \boldsymbol{J}^{-1} \begin{bmatrix} \Delta P \\ \Delta Q \end{bmatrix} \tag{28}$$

$$\boldsymbol{S} = \boldsymbol{J}^{-1} = \begin{bmatrix} S_{\theta P} & S_{\theta Q} \\ S_{UP} & S_{UQ} \end{bmatrix} \tag{29}$$

where $\Delta\theta$ and ΔU are decoupled in (28) and (29). ΔU can be calculated as

$$\Delta U = S_{UP} \cdot \Delta P + S_{UQ} \cdot \Delta Q \tag{30}$$

The reactive and active power are sequentially operated in the real-time operation; thus, $\boldsymbol{\Delta Q}$ and $\boldsymbol{\Delta P}$ can be separated into

$$\boldsymbol{\Delta Q}(t) = S_{UQ}^{-1}(t) \cdot \Delta U(t) \tag{31}$$

$$\boldsymbol{\Delta P}(t) = S_{UP}^{-1}(t) \cdot \Delta U(t) \tag{32}$$

where $\Delta U(t) = \left[\Delta U^1(t), \ldots, \Delta U^i(t), \ldots, \Delta U^{N_c}(t)\right]^{\text{T}}$. It denotes the voltage difference between customers' node and the high or low limit. The voltage difference of customer i of phase p at time slot t is as follows:

$$\Delta U^{i,p}(t) = \begin{cases} U^{i,p}(t) - V_{\max}, & U^{i,p}(t) > V_{\max} \\ U^{i,p}(t) - V_{\min}, & U^{i,p}(t) < V_{\min} \\ 0, & \text{others} \end{cases} \tag{33}$$

The matrices $\boldsymbol{\Delta Q}(t)$ and $\boldsymbol{\Delta P}(t)$ are the required reactive and active power that used to adjust the voltage to the allowable ranges. At the beginning of each time slot, when the voltage violation is observed, each sub-CEMS searches and operates the available reactive or active power according to $\boldsymbol{\Delta Q}(t)$ or $\boldsymbol{\Delta P}(t)$, respectively. For example, in an under-voltage condition, the active power that needs to turn off at customer i of phase p is $\Delta P^{i,p}(t)$. The available active power of customer i will be searched first, and then a value list of power is generated with different combination of available FRs. Finally, the larger and closest value to $\Delta P^{i,p}(t)$ will be chosen. The available FRs mean that the FRs are on-working, can be interrupted, and still have enough time to finish their work. In other words, the above-mentioned constraints of the FRs are considered in the real-time operation.

4 Case studies

4.1 Test system and parameters

As shown in Fig. 3, the proposed method is validated using a typical three-phase unbalanced distribution system, which serves 1800-customers. In this system, there are five primary nodes under the substation transformer. Under each primary node, there are 30 pole transformers. The pole transformers distribute power to customers with three phases. Customers are equally divided into three groups and randomly connected with phase a or b or c. Each customer is installed with a PV generation and an EV in the case studies. The data for the PVs and loads are obtained from the demonstration project conducted by the New Energy and Industrial Technology Development Organisation in Ota City, Japan [30]. The load data for each customer includes the ODL and the FL. The real load data is utilised for ODL. Six most commonly used FRs are assumed, which is shown in Table 1. The models of FLs such as rice cooker, washing machine are assumed as a load that consume a certain volume of energy during an allowable interval [21, 35]. The power of the EVs is assumed as 4 kW during the charging. The study is performed based on the data for 30 days in June. Among these days, the aggregated data of PV peak of all the 1800 customers is 5.78 MW, while the load peak is 6.72 MW.

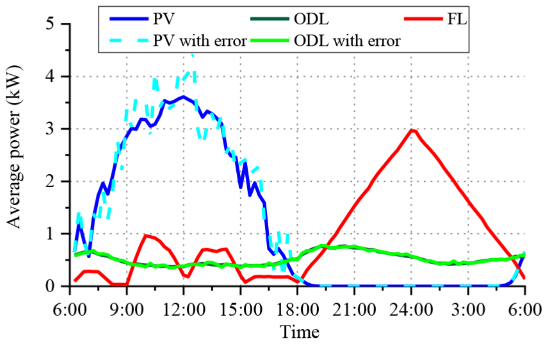

Fig. 4 *PV and load average data of 2nd June*

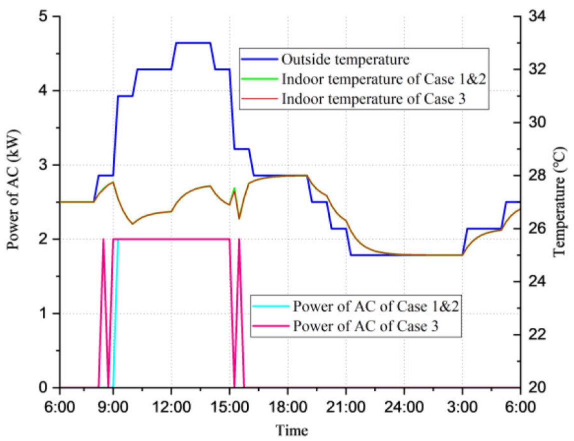

Fig. 5 *Temperature and power of AC at customer node 35*

Fig. 4 illustrates the average data of PV, ODL, and FR on 2nd June of all the 1800 customers.

The start time of FRs is randomly decided. The curve of FR is a triangle shape since the EV power curve is a normal distribution. 2nd June is a sunny day, the PV output is high with small fluctuation. We assume that there are some errors in the day-ahead forecasted data. However, the forecast method is out of the scope of this study. Moreover, the day-ahead electricity price is adopted from the Nord Pool market in Denmark in June 2016 [36]. The duration of the time slot is 15 min for the day-ahead optimisation and 5 min for the real-time operation, respectively. In Japan, the voltage limitation is [95,107] V. The GA parameters of the population, crossover rate, mutation rate, and generation are 20, 0.8, 0.02, and 2000, respectively. The simulation is performed using MATLAB software on a computer with a central processing unit of Intel(R) Core(TM) i5-6500 @ 3.20 GHz and 4 GB memory.

Four cases are considered in the day-ahead scheduling.

Case 1: The FRs cannot provide regulation services. The customers' electricity cost and the system voltage are not optimised.
Case 2: The customers' electricity cost is minimised without voltage regulation.
Case 3: Both the customers' electricity cost and the voltage violation times are optimised.
Case 4: Comparison with a centralised optimisation method [31].

4.2 Analysis of results

2nd June is taken as a typical day for illustrating the effect of FR utilisation. The output of the OLTC is set as 1.025 p.u. at the beginning, and the change ratio per step is set as 0.0125 p.u.. The calculation time for day-ahead scheduling and real-time operation of a sub-CEMS are ∼5.8 min and 0.017 s, respectively.

The outside temperature is shown with the blue curve in Fig. 5. The comfortable range of indoor temperature is set as [24, 28]°C. Since the temperature is higher than 28°C during the daytime, the AC is started for cooling. The power of the AC operation of Cases 1 and 2 is shown in the cyan curve. When the indoor temperature is in a comfortable range, the AC can be utilised for over-voltage mitigation. Thus, the pink curve of Case 3 has some differences from Cases 1 and 2 around 9:00.

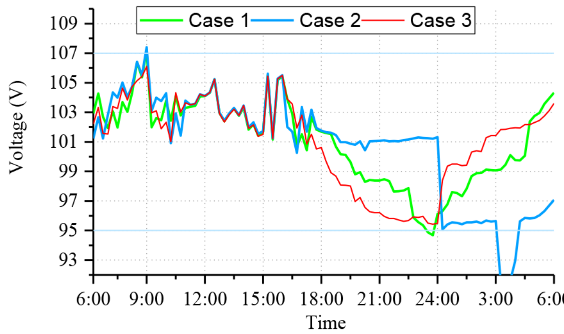

Fig. 6 *Voltage at customer node 35 of the three cases*

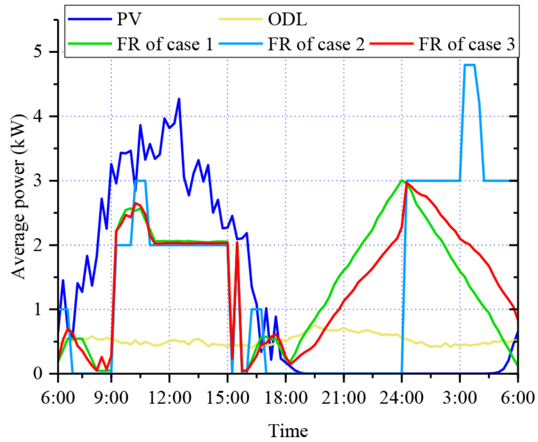

Fig. 7 *Average power of PV and load of the three cases*

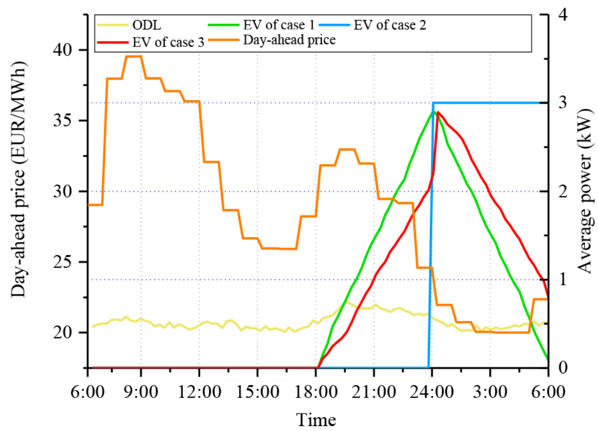

Fig. 8 *Price, average power of EV for the three cases*

The voltage of customer 35 of the three cases is shown in Fig. 6. It can be seen that the voltages are higher than the upper limit around 9:00 in Cases 1 and 2. Within the operation of AC, the over-voltage can be mitigated in Case 3.

Fig. 7 shows the average power of PV and load of the three cases. In Case 1, FRs are randomly started, indicating a normal situation and FRs are not scheduled. The power consumption in Case 1 is a normal distribution, which is triangular in shape from 18:00 to 6:00. In Case 2, the scheduling of FRs is only to minimise the customers' cost. Thus, FRs are all operated during the low price period of their allowable interval, creating high load peaks. In contrast, in Case 3, the scheduling of FRs considers both the minimisation of customers' cost and voltage violations. As a result, the load peak is much lower than Case 2.

Specifically, Fig. 8 illustrates the electricity price and the operation power of EVs in the three cases. All EVs are charged from 24:00 to 6:00 because of the low price in Case 2. In Case 3,

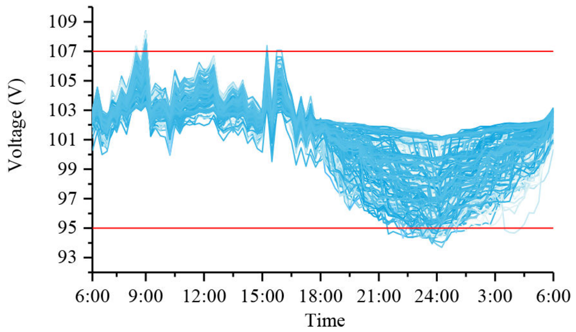

Fig. 9 *Day-ahead voltage of the 600 customers of Case 1*

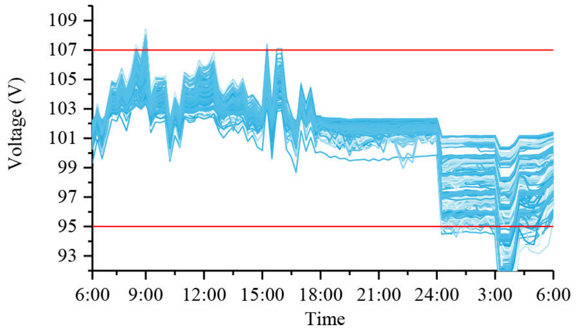

Fig. 10 *Day-ahead voltage of the 600 customers of Case 2*

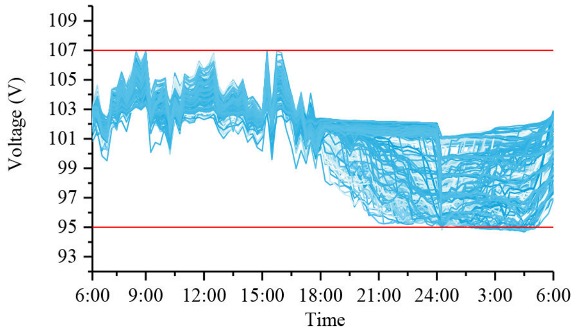

Fig. 11 *Day-ahead voltage of the 600 customers of Case 3*

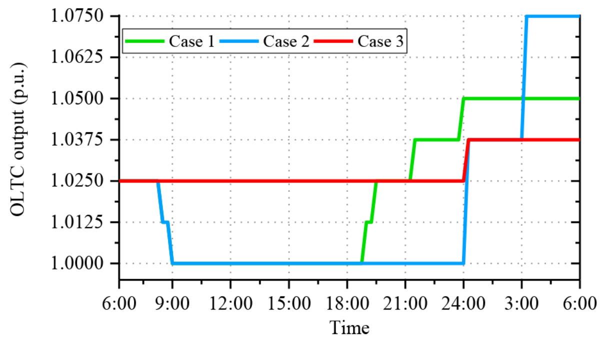

Fig. 12 *Day-ahead schedule of the OLTC*

only a few EVs are arranged to charge at the low price period comparing to Case 2, making the load peak lower than Case 2.

The day-ahead voltage condition of phase *a* of the three cases is shown in Figs. 9–11. Each shade of a blue curve indicates a voltage condition of 24 h of a customer node. In Fig. 9, over-voltage violations occur around 9:00 and 16:00 in Case 1, when the PV output is more than 2 kW and the AC is not working, i.e. reverse power is large at the time. Under-voltage violations occur around 24:00 when the load peak is high. In Fig. 10, the under-voltage problem is serious because of the high load peak from 24:00 to 6:00 in Case 2. In Fig. 11, it can be seen that all the over-voltage violations are mitigated by the starting of ACs. The under-voltage problem is relatively small compared to Cases 1 and 2 because the scheduling of FRs considers the voltage violation times minimisation.

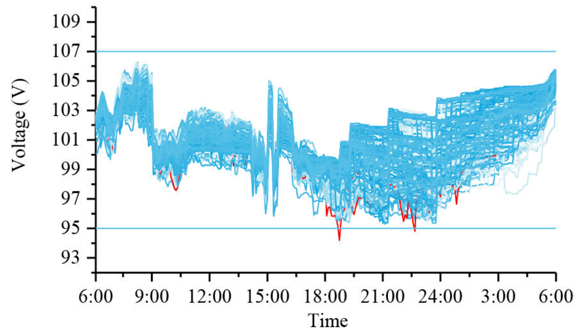

Fig. 13 *Real-time voltage of the 600 customers of Case 1*

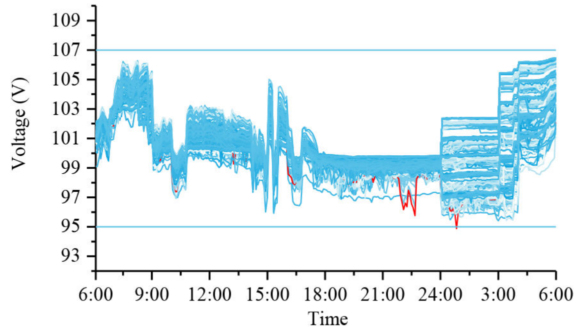

Fig. 14 *Real-time voltage of the 600 customers of Case 2*

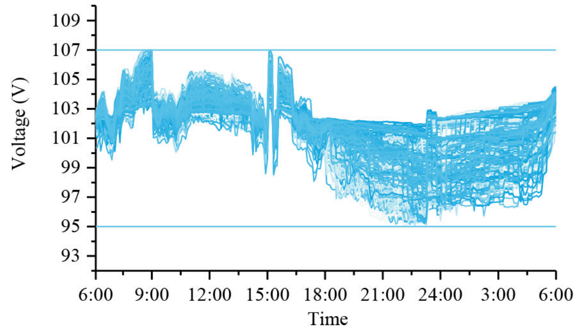

Fig. 15 *Real-time voltage of the 600 customers of Case 3*

Fig. 12 shows the day-ahead scheduling of OLTC operation for the three cases that can regulate the voltage to the permissible ranges. The OLTC tap operation numbers for Cases 1, 2, and 3 are 6, 8, and 1, respectively. Since the over- and under-voltage violations are serious in Cases 1 and 2. The OLTC needs frequent operation to regulate the voltage to the permissible range. Compared with Cases 1 and 2, it reveals that if the FLs are scheduled only for reducing the electricity cost, the OLTC operation number will increase because of the serious voltage violations. In Case 3, the OLTC operation number is largely reduced compared with Cases 1 and 2.

Figs. 13–15 illustrate the real-time voltage condition of phase *a* of the 600 customers. It can be seen that in Cases 1 and 2, even with the frequent operation of OLTC, the voltage violations still occur in the real-time scale. Since the errors are inevitable in the day-ahead scheduling. In Cases 1 and 2, more OLTC operation or other voltage regulation method should be applied to control the voltage in real-time. With the proposed real-time operation method, the voltage is regulated to the permissible range in Case 3, as shown in Fig. 15.

Fig. 16 shows the voltage of phases *a*, *b* and *c*. Since the PV generation and loads of each customer are different, voltages of each phase also have some differences. This result indicate that the scheduling of FLs should consider the modelling of unbalanced networks, as a balanced representation using the average voltage value may not capture some of the voltage violations.

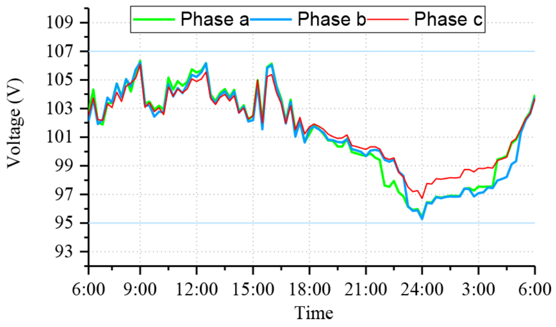

Fig. 16 *Voltage of phases a, b and c of primary node 5*

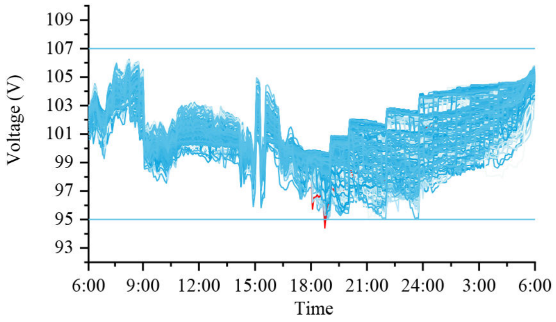

Fig. 17 *Real-time voltage of the 600 customers of Case 4*

4.3 Comparison with a centralised optimisation

The proposed method is also compared with a centralised method of [31]. Ziadi *et al*. [31] proposes a centralised day-ahead scheduling for PVs, battery energy storage system, controller loads and OLTC. The objectives are to achieve loss reduction, voltage regulation and smoothing the power flow. The optimisation is based on estimated data of load and PV. The simulation is carried out with the time interval of 1 h in a 15-bus radial power distribution system.

However, applying the method of [31] to our model, the solution space becomes the start time of 1800 customers' FRs, the PVs' reactive power, and the OLTC tap setting during the 96-time slots of a day. In other words, the solution space is getting much larger. Since the schedule of FRs and OLTC are highly correlated. The power flow calculation is time-consuming, and the technique in [31] cannot achieve acceptable results after 24 h of simulation.

To simplify the simulation, the OLTC operation is separated from the FR scheduling, and then a centralised optimisation is performed on 2nd June according to [31]. The day-ahead voltage condition of phase *a* and the OLTC operation are similar to Case 1, indicating that over- and under-voltage violations are not avoided in the centralised optimisation of FRs. The OLTC still needs to operate frequently to regulate the voltage violations. Furthermore, under-voltage violation still occurs one time in a real-time scale, which is shown in Fig. 17. It indicates that (i) the centralised optimisation of a large-scale system cannot be well solved. (ii) voltage violations occur in real-time operation due to forecasted errors.

Compared with the method in [31], the improvements are as follows. We propose two-stage control, where the real-time operation can solve the errors of day-ahead estimated data and ensure the node voltage to be within the allowable ranges. Moreover, the optimisation scheduling of FRs in a large-scale distribution system is solved by each sub-CEMS separately. As a result, the optimisation can achieve a better result.

The real-time operations of OLTC of the four cases are shown in Fig. 18. Compared with Fig. 12, it can be seen that the OLTC needs more operations in order to eliminate the under-voltage in Case 1 and Case 2. However, the high value output of OLTC (i.e. larger than 1.0625 p.u.) would cause over-voltage easily. As a result, the OLTC needs to decrease the tap before 6:00 of the next day.

In short, the numbers of voltage violation, OLTC tap operation in day-ahead and real-time scales are concluded in Table 2. It

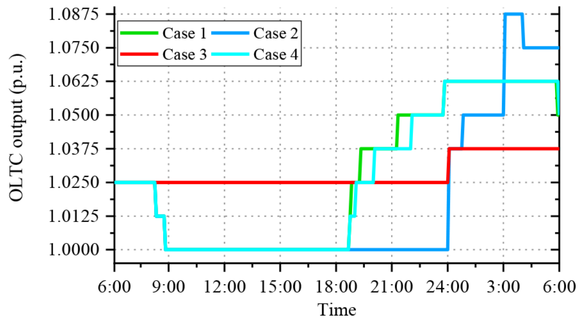

Fig. 18 *Real-time operation of the OLTC*

Table 2 Times of voltage violations and OLTC operations of the four cases

Case name	Times of voltage violations		Times of OLTC tap operation	
	Day-ahead	Real-time	Day-ahead	Real-time
Case 1	289	2	6	8
Case 2	1412	1	8	10
Case 3	91	0	1	1
Case 4	166	1	6	8

should be noted that when accounting voltage violations, an over- or under-voltage in a node of a time slot is counted as 1. The number of violations is the summation of the over- or under-voltages. In Case 3, the OLTC only needs to operate once with the assistance of FRs' scheduling, where all the voltage violations can be mitigated. The pressure of OLTC operation can be greatly decreased in Case 3 compared to the other cases.

5 Discussions

Although current rooftop PVs do not generally contribute to voltage control, and most of them are not controlled by DSO, a lot of studies focus on utilising PVs for solving the over-voltage problem. A bi-directional control signal from a central/hierarchical hub is needed to control the FRs, which seems challenging at present. However, with the rapid development of ICTs, PVs and smart loads are connected to the internet, which can be communicated and controlled with almost no time delay with the 5G technology [17]. As a result, the bi-directional control of FRs is practicable in the near future.

In some areas of the world, DR program such as load shifting is already implemented. Customers are encouraged to provide their FRs, such as ACs [37], to support the operation of the power grid. Customers can get some profit from the DR program without disturbing their comfort. Figs. 12 and 18 show that, traditional voltage regulation devices have more pressure to cope with the voltage fluctuation caused by high penetration of PVs and EVs. It will be advantageous for DSO to introduce the FRs for the voltage regulation, especially when FRs are already utilised in the DR program.

6 Conclusions

The DR with the progressed information communication techniques is attracting attention in the application of smart grids. The utilisation of customers' FRs could flatten the power demand curve as well as stabilise the distribution voltage condition. In this paper, a two-stage voltage regulation technique is proposed by utilising the FRs. The first stage is the day-ahead scheduling, which optimally schedules the start time of FRs to minimise the electricity cost of customers and network voltage violation times. The second stage is the real-time operation, where the shifting method of FRs is proposed to ensure the voltage within the permissible range. The simulation results illustrate that the OLTC needs eight or ten times of operations, respectively, in order to regulate the voltage to the permissible range, if the FRs are not scheduled or scheduled only for reducing the electricity cost. It is a tough situation for DSOs because the excessive operation of OLTC should be avoided. In contrast, if the FRs can be utilised through DR, the operation number of OLTC can be decreased to only one time. This greatly relieves the regulation stress of the DSOs. Future work should design mechanisms for encouraging and rewarding customers to contribute their FRs in voltage regulation.

7 References

[1] Ipakchi, A., Albuyeh, F.: 'Grid of the future', *IEEE Power Energy Mag.*, 2009, **7**, (2), pp. 52–62

[2] Ueda, Y., Kurokawa, K., Tanabe, T., *et al.*: 'Analysis results of output power loss due to the grid voltage rise in grid-connected photovoltaic power generation systems', *IEEE Trans. Ind. Electron.*, 2008, **55**, (2), pp. 2744–2751

[3] Mou, Y., Xing, H., Lin, Z., *et al.*: 'Decentralized optimal demand-side management for PHEV charging in a smart grid', *IEEE Trans. Smart Grid*, 2015, **6**, (2), pp. 726–736

[4] Clement-Nyns, K., Haesen, E., Driesen, J.: 'The impact of charging plug-in hybrid electric vehicles on a residential distribution grid', *IEEE Trans. Power Syst.*, 2010, **25**, (1), pp. 371–380

[5] Long, C., Ochoa, L.F.: 'Voltage control of PV-rich LV networks: OLTC-fitted transformer and capacitor banks', *IEEE Trans. Power Syst.*, 2016, **31**, (5), pp. 4016–4025

[6] Thomson, M.: 'Automatic-voltage-control relays and embedded generation', *Power Eng. J.*, 2000, **14**, (2), pp. 71–76

[7] Ibrahim, M., Salama, M.M.A.: 'Smart distribution system volt/VAR control using distributed intelligence and wireless communication', *IET Gener. Transm. Distrib.*, 2015, **9**, (4), pp. 307–318

[8] Homaee, O., Zakariazadeh, A., Jadid, S.: 'Real-time voltage control algorithm with switched capacitors in smart distribution system in presence of renewable generations', *Int. J. Electr. Power Energy Syst.*, 2014, **54**, pp. 187–197

[9] Hussain, I., Das, D.C., Sinha, N.: 'Reactive power performance analysis of dish-stirling solar thermal-diesel hybrid energy system', *IET Renew. Power Gener.*, 2017, **11**, (6), pp. 750–762

[10] Demirok, E., Gonz, P. C., Frederiksen, K. H. B., *et al.*: 'Local reactive power control methods for overvoltage prevention of distributed solar inverters in low-voltage grids', *IEEE J. Photovoltaics*, 2011, **1**, (2), pp. 174–182

[11] Deshmukh, S., Natarajan, B., Pahwa, A.: 'Voltage/VAR control in distribution networks via reactive power injection through distributed generators', *IEEE Trans. Smart Grid*, 2012, **3**, (3), pp. 1226–1234

[12] Carvalho, P.M.S., Correia, P.F., Ferreira, L.A. F.: 'Distributed reactive power generation control for voltage rise mitigation in distribution networks', *IEEE Trans. Power Syst.*, 2008, **23**, (2), pp. 766–772

[13] Daratha, N., Das, B., Sharma, J.: 'Coordination between OLTC and SVC for voltage regulation in unbalanced distribution system distributed generation', *IEEE Trans. Power Syst.*, 2014, **29**, (1), pp. 289–299

[14] Salih, S.N., Chen, P.: 'On coordinated control of OLTC and reactive power compensation for voltage regulation in distribution systems with wind power', *IEEE Trans. Power Syst.*, 2016, **31**, (5), pp. 4026–4035

[15] Muttaqi, K.M., Le, A.D.T., Negnevitsky, M., *et al.*: 'A coordinated voltage control approach for coordination of OLTC, voltage regulator, and DG to regulate voltage in a distribution feeder', *IEEE Trans. Ind. Appl.*, 2015, **51**, (2), pp. 1239–1248

[16] Hashemi, S., Østergaard, J.: 'Methods and strategies for overvoltage prevention in low voltage distribution systems with PV', *IET Renew. Power Gener.*, 2017, **11**, (2), pp. 205–214

[17] Hui, H., Ding, Y., Shi, Q., *et al.*: '5G network-based internet of things for demand response in smart grid: a survey on application potential', *Appl. Energy*, 2020, **257**, p. 113972

[18] Mohsenian-Rad, A.H., Wong, V.W.S., Jatskevich, J., *et al.*: 'Autonomous demand-side management based on game-theoretic energy consumption scheduling for the future smart grid', *IEEE Trans. Smart Grid*, 2010, **1**, (3), pp. 320–331

[19] Dupont, B., Dietrich, K., De Jonghe, C., *et al.*: 'Impact of residential demand response on power system operation: a Belgian case study', *Appl. Energy*, 2014, **122**, pp. 1–10

[20] Barik, A.K., Das, D.C.: 'Proficient load-frequency regulation of demand response supported bio-renewable cogeneration based hybrid microgrids with quasi-oppositional selfish-herd optimisation', *IET Gener. Transm. Distrib.*, 2019, **13**, (13), pp. 2889–2898

[21] Zhao, Z., Lee, W.C., Shin, Y., *et al.*: 'An optimal power scheduling method for demand response in home energy management system', *IEEE Trans. Smart Grid*, 2013, **4**, (3), pp. 1391–1400

[22] Barik, A.K., Das, D.C.: 'Coordinated regulation of voltage and load frequency in demand response supported biorenewable cogeneration–based isolated hybrid microgrid with quasi-oppositional selfish herd optimisation', *Int. Trans. Electr. Energy Syst.*, 2019, **30**, (1), pp. 1–22

[23] Liu, X., Aichhorn, A., Liu, L., *et al.*: 'Coordinated control of distributed energy storage system with tap changer transformers for voltage rise mitigation under high photovoltaic penetration', *IEEE Trans. Smart Grid*, 2012, **3**, (2), pp. 897–906

[24] Calderaro, V., Galdi, V., Lamberti, F., *et al.*: 'A smart strategy for voltage control ancillary service in distribution networks', *IEEE Trans. Power Syst.*, 2015, **30**, (1), pp. 494–502

[25] Tonkoski, R., Lopes, L.A.C., El-Fouly, T.H.M.: 'Coordinated active power curtailment of grid connected PV inverters for overvoltage prevention', *IEEE Trans. Sustain. Energy*, 2011, **2**, (2), pp. 139–147

[26] Vivekananthan, C., Mishra, Y., Ledwich, G., *et al.*: 'Demand response for residential appliances via customer reward scheme', *IEEE Trans. Smart Grid*, 2014, **5**, (2), pp. 809–820

[27] Venkatesan, N., Solanki, J., Solanki, S.K.: 'Residential demand response model and impact on voltage profile and losses of an electric distribution network', *Appl. Energy*, 2012, **96**, pp. 84–91

[28] Shi, W., Li, N., Xie, X., *et al.*: 'Optimal residential demand response in distribution networks', *IEEE J. Sel. Areas Commun.*, 2014, **32**, (7), pp. 1441–1450

[29] O'Connell, A., Flynn, D., Keane, A.: 'Rolling multi-period optimization to control electric vehicle charging in distribution networks', *IEEE Trans. Power Syst.*, 2014, **29**, (1), pp. 340–348

[30] Xie, Q., Hara, R., Kita, H., *et al.*: 'Coordinated control of OLTC and multi-CEMSs for overvoltage prevention in power distribution system', *IEEJ Trans. Electr. Electron. Eng.*, 2017, **12**, (5), pp. 692–701

[31] Ziadi, Z., Taira, S., Oshiro, M., *et al.*: 'Optimal power scheduling for smart grids considering controllable loads and high penetration of photovoltaic generation', *IEEE Trans. Smart Grid*, 2014, **5**, (5), pp. 2350–2359

[32] Burger, S., Chaves-Ávila, J.P., Batlle, C., *et al.*: 'A review of the value of aggregators in electricity systems', *Renew. Sustain. Energy Rev.*, 2017, **77**, pp. 395–405

[33] Wang, S., Chen, S., Ge, L., *et al.*: 'Distributed generation hosting capacity evaluation for distribution systems considering the robust optimal operation of OLTC and SVC', *IEEE Trans. Sustain. Energy*, 2016, **7**, (3), pp. 1111–1123

[34] Olivier, F., Aristidou, P., Ernst, D., *et al.*: 'Active management of low-voltage networks for mitigating overvoltages due to photovoltaic units', *IEEE Trans. Smart Grid*, 2016, **7**, (2), pp. 926–936

[35] Yao, E., Samadi, P., Wong, V.W.S., *et al.*: 'Residential demand Side management under high penetration of rooftop photovoltaic units', *IEEE Trans. Smart Grid*, 2016, **7**, (3), pp. 1597–1608

[36] 'Day-ahead price data of Denmark1', http://www.nordpoolspot.com/Market-data1/Elspot/Area-Prices/ALL1/Hourly/?view=chart, 2016

[37] Hui, H., Ding, Y., Liu, W., *et al.*: 'Operating reserve evaluation of aggregated air conditioners', *Appl. Energy*, 2017, **196**, pp. 218–228